Published in final edited form as:
*Nature*. 2011 March 24; 471(7339): 508–512. doi:10.1038/nature09867.

# Fat cells reactivate quiescent neuroblasts via TOR and glial Insulin relays in *Drosophila*

**Rita Sousa-Nunes**, **Lih Ling Yee**, and **Alex P. Gould***
Division of Developmental Neurobiology, Medical Research Council National Institute for Medical Research, The Ridgeway, Mill Hill, London NW7 1AA, UK

## Abstract

Many stem, progenitor and cancer cells undergo periods of mitotic quiescence from which they can be reactivated[1-5]. The signals triggering entry into and exit from this reversible dormant state are not well understood. In the developing *Drosophila* central nervous system (CNS), multipotent self-renewing progenitors called neuroblasts[6-9] undergo quiescence in a stereotypical spatiotemporal pattern[10]. Entry into quiescence is regulated by Hox proteins and an internal neuroblast timer[11-13]. Exit from quiescence (reactivation) is subject to a nutritional checkpoint requiring dietary amino acids[14]. Organ co-cultures also implicate an unidentified signal from an adipose/hepatic-like tissue called fat body[14]. Here, we provide *in vivo* evidence that Slimfast amino-acid sensing and Target-of-Rapamycin (TOR) signalling[15] activate a fat-body derived signal (FDS) required for neuroblast reactivation. Downstream of the FDS, Insulin-like receptor (InR) signalling and the Phosphatidylinositol 3-Kinase (PI3K)/TOR network are required in neuroblasts for exit from quiescence. We demonstrate that nutritionally regulated glial cells provide the source of Insulin-like Peptides (Ilps) relevant for timely neuroblast reactivation but not for overall larval growth. Conversely, Ilps secreted into the hemolymph by median neurosecretory cells (mNSCs) systemically control organismal size[16-18] but do not reactivate neuroblasts. *Drosophila* thus contains two segregated Ilp pools, one regulating proliferation within the CNS and the other controlling tissue growth systemically. Together, our findings support a model in which amino acids trigger the cell cycle re-entry of neural progenitors via a fat body→glia→neuroblasts relay. This mechanism highlights that dietary nutrients and remote organs, as well as local niches, are key regulators of transitions in stem-cell behaviour.

In fed larvae, *Drosophila* neuroblasts (Fig. 1a) exit quiescence from the late first instar (L1) stage onwards. This reactivation involves cell enlargement and entry into S-phase, monitored in this study using the thymidine analogue, 5-ethynyl-2′-deoxyuridine (EdU). Consistent with a previous study[10], we observed that reactivated neuroblast lineages (neuroblasts and their progeny, Fig 1b) reproducibly incorporated EdU in a characteristic spatiotemporal sequence: central brain (CB) → thoracic (Th) → abdominal (Ab) neuromeres (Fig. 1c and Supplementary Fig. 1). Mushroom-body neuroblasts (MB NBs) and one ventrolateral neuroblast, however, are known not to undergo quiescence and to continue dividing for several days in the absence of dietary amino acids[14] (Fig. 1a,c,f). This indicates that dietary amino acids are more than mere “fuel”, providing a specific signal that reactivates neuroblasts. However, explanted CNSs incubated with amino acids do not

*To whom correspondence and requests for materials should be addressed to A.P.G.: agould@nimr.mrc.ac.uk.

**Author contributions**
R.S.-N. and A.P.G. designed the experiments, R.S.-N and L.L.Y. performed the experiments and R.S.-N. and A.P.G. wrote the manuscript. All authors have read and subscribe to the contents of the manuscript.

**Competing Interest Statement:** the authors declare that they have no competing financial interests.


Europe PMC Funders Author Manuscripts

undergo neuroblast reactivation unless co-cultured with fat body from larvae raised on a diet containing amino acids[14]. We therefore tested the *in vivo* requirement for a fat-body derived signal (FDS) in neuroblast reactivation by blocking vesicular trafficking and thus signalling from this organ using a dominant-negative Shibire Dynamin ($Shi^{DN}$). This strongly reduced EdU neuroblast incorporation, indicating that exit from quiescence *in vivo* requires a FDS (Fig. 1d,e). One candidate we tested was *Ilp6*, known to be expressed by the fat body[19, 20], but neither fat-body specific overexpression nor RNA interference of this gene significantly affected neuroblast reactivation (Supplementary Table 1 and data not shown). Fat body cells are known to sense amino acids via the cationic amino-acid transporter Slimfast (Slif), which activates the TOR signalling pathway, in turn leading to the production of a systemic growth signal[15, 21]. We found that fat-body specific overexpression of the TOR activator, Ras Homologue Enriched in Brain (Rheb) or of an activated form of the p110 PI3K catalytic subunit, or of the p60 adaptor subunit, had no significant effect on neuroblast reactivation in fed animals or in larvae raised on a nutrient-restricted (NR) diet lacking amino-acids (Fig. 1e,f and data not shown). In contrast, global inactivation of *Tor*, fat-body specific *Slif* knockdown or fat-body specific expression of the TOR inhibitors Tuberous Sclerosis Complex 1 and 2 (TSC1/2) all strongly reduced neuroblasts from exiting quiescence (Fig. 1d,e). These results together show that a Slif/TOR-dependent FDS is required for neuroblasts to exit quiescence and that this may be equivalent to the FDS known to regulate larval growth.

We next investigated the signalling pathways essential within neuroblasts for their reactivation. Nutrient-dependent growth is regulated in many species by the interconnected TOR and PI3K pathways[22-24] (Supplementary Fig. 2). In fed larvae, we found that neuroblast inactivation of TOR signalling (by overexpression of TSC1/2), or PI3K signalling (by overexpression of p60, the Phosphatase and Tensin homologue PTEN, the Forkhead box subgroup O transcription factor FoxO or dominant-negative p110), all inhibited reactivation (Fig. 1e). Conversely, stimulation of neuroblast TOR signalling (by overexpression of Rheb) or PI3K signalling (by overexpression of activated p110 or Phosphoinositide-Dependent Kinase 1, PDK1) triggered precocious exit from quiescence (Fig. 1e). Rheb overexpression had a particularly early effect, preventing some neuroblasts from undergoing quiescence even in newly hatched larvae (Supplementary Fig. 3). Hence, TOR/PI3K signalling in neuroblasts is required to trigger their timely exit from quiescence. Importantly, neuroblast overexpression of Rheb or activated p110 in NR larvae, which lack FDS activity[14], was sufficient to bypass the NR block to neuroblast reactivation (Fig. 1f). Strikingly, both genetic manipulations were even sufficient to reactivate neuroblasts in explanted CNSs, cultured without fat body or any other tissue (Fig. 1g). Together with the previous results, this indicates that neuroblast TOR/PI3K signalling lies downstream of the amino-acid dependent FDS during exit from quiescence.

To identify the mechanism bridging the FDS with neuroblast TOR/PI3K signalling, we tested the role of the Insulin-like Receptor (InR, Supplementary Fig. 2). Importantly, a dominant-negative InR inhibited neuroblast reactivation whereas an activated form stimulated premature exit from quiescence (Fig. 1e). Furthermore, InR activation was sufficient to bypass the NR block to neuroblast reactivation (Fig. 1f). This suggests that at least one of the potential InR ligands, the seven Insulin-like peptides (Ilps), may be the neuroblast reactivating signal(s). By testing various combinations of targeted *Ilp* null alleles[25] and genomic *Ilp* deficiencies[25, 26], we found that neuroblast reactivation was moderately delayed in larvae deficient for both *Ilp2* and *Ilp3* (*Df[Ilps2-3]*) or lacking *Ilp6* activity (Fig. 2a). Stronger delays, as severe as those observed in $InR^{31}$ mutants, were observed in larvae simultaneously lacking the activities of *Ilp2*, *Ilp3* and *Ilp5* (*Df[Ilps2-3],Ilp5*) or *Ilps1-5* (*Df[Ilps1-5]*) (Fig. 2a). Despite the developmental delay in *Df[Ilps1-5]* animals[25, 26], neuroblast reactivation eventually begins in the normal spatial

pattern albeit heterochronically, in larvae with L3 morphology (Fig. 2b, compare timeline with Fig. 1c). Together, the genetic analysis shows that Ilps 2, 3, 5 and 6 regulate the timing but not the spatial pattern of neuroblast exit from quiescence. However, as removal of some Ilps can induce compensatory regulation of others[25], the relative importance of each cannot be assessed from loss-of-function studies alone.

Brain mNSCs (Fig. 1a) are an important source of Ilps, secreted into the hemolymph in an FDS-dependent manner to regulate larval growth[16-18, 21]. They express *Ilp1, Ilp2, Ilp3* and *Ilp5*, although not all during the same development stages[16-18]. However, we found that none of the seven Ilps could reactivate neuroblasts during NR when overexpressed in mNSCs (Supplementary Table 2). Similarly, increasing mNSC secretion using the NaChBac sodium channel[21] or altering mNSC size using PI3K inhibitors/activators, which in turn alters body growth, did not significantly affect neuroblast reactivation under fed conditions (Fig. 2a,c, Supplementary Fig. 1b and L. Cheng, A. Bailey, S. Leevers, T. Ragan, P. Driscoll & A.P.G, submitted). Surprisingly, therefore, mNSCs are not the relevant Ilp source for neuroblast reactivation. Nonetheless, *Ilp3* and *Ilp6* mRNAs were detected in the CNS cortex, at the early L2 stage, in a domain distinct from the *Ilp2*$^{+}$ mNSCs (Supplementary Fig. 4). Two different *Ilp3-lacZ* transgenes[17] suggest that *Ilp3* is expressed in some glia (Repo$^{+}$ cells) and neurons (Elav$^{+}$ cells). An *Ilp6-GAL4* insertion (see Methods) suggests that *Ilp6* is also expressed in glia, including the cortex glia surrounding neuroblasts and the surface glia of the blood-brain-barrier (BBB) (Fig. 3a).

We next assessed the ability of each of the seven Ilps to reactivate neuroblasts when overexpressed in glia or in neurons (Supplementary Table 2). Pan-glial or pan-neuronal overexpression of Ilp4, Ilp5 or Ilp6 led to precocious reactivation under fed conditions (Fig. 3b,c). Each of these manipulations also bypassed the NR block to neuroblast reactivation, as did overexpression of Ilp2 in glia or in neurons, or Ilp3 in neurons (Fig. 3d and Supplementary Table 2). In all of these Ilp overexpressions, and even when Ilp6 was expressed in the posterior *Ultrabithorax* (*Ubx*) domain (Fig. 3e), the temporal rather than the spatial pattern of reactivation was affected. Importantly, experiments blocking cell signalling with Shi$^{DN}$ indicate that glia rather than neurons are critical for neuroblast reactivation (Fig. 4a,b). Interestingly, glial-specific overexpression of Ilps 3-6 did not significantly alter larval mass (Fig. 2c). Thus, in contrast to mNSC-derived Ilps, glial-derived Ilps promote CNS growth without affecting body growth.

Focusing on Ilp6, we used CNS explant cultures to demonstrate directly that glial overexpression was sufficient to substitute for the FDS during neuroblast exit from quiescence (Fig. 3d). *In vivo*, Ilp6 was sufficient to induce reactivation during NR when overexpressed via its own promoter or specifically in cortex glia but not in the subperineurial BBB glia, nor in many other CNS cells that we tested (Fig. 3d and Supplementary Table 1). Hence, cortex glia possess the appropriate processing machinery and/or location to deliver reactivating Ilp6 to neuroblasts. *Ilp6* mRNA is known to be up- rather than down-regulated in the larval fat body during starvation[19] and, accordingly, *Ilp6-GAL4* activity is increased in this tissue following NR (Fig. 4c). Conversely, we found that *Ilp6-GAL4* is strongly downregulated in CNS glia during NR (Fig. 4c). Thus, dietary nutrients stimulate glia to express *Ilp6* at the transcriptional level. Consistent with this, an important transducer of nutrient signals, the TOR/PI3K network, is necessary and sufficient in glia (but not in neurons) for neuroblast reactivation (Fig. 4a,b). Together, the genetic and expression analyses indicate that nutritionally regulated glia relay the FDS to quiescent neuroblasts via Ilps.

This study used an integrative physiology approach to identify the relay mechanism regulating a nutritional checkpoint in neural progenitors. A central feature of the fat

body→glia→neuroblasts relay model is that glial Insulin signalling bridges the amino-acid/TOR-dependent FDS with InR/PI3K/TOR signalling in neuroblasts (Fig. 4d). The importance of glial Ilp signalling during neuroblast reactivation is also underscored by an independent study, published while this work was under revision[27]. As TOR signalling is also required in neuroblasts and glia, direct amino-acid sensing by these cell types may also impinge upon the linear tissue relay. This would then constitute a feed-forward persistence detector[28], ensuring that neuroblasts exit quiescence only if high amino-acid levels are sustained rather than transient. We also showed that the CNS "compartment" in which glial Ilps promote growth is functionally isolated, perhaps by the blood-brain barrier, from the systemic compartment where mNSC Ilps regulate the growth of other tissues. The existence of two functionally separate Ilp pools may explain why bovine Insulin cannot reactivate neuroblasts in CNS organ culture[14], despite being able to activate *Drosophila* InR *in vitro*[29]. Given that Insulin/PI3K/TOR signalling components are highly conserved between insects and vertebrates, it will be important to address whether mammalian adipose or hepatic tissues signal to glia and whether or not this involves an Insulin/IGF relay to CNS progenitors. In this regard, it is intriguing that brain-specific overexpression of IGF1 can stimulate cell-cycle re-entry of mammalian cortical neural progenitors[30], suggesting utilization of at least part of the mechanism identified here in *Drosophila*.

## METHODS SUMMARY

For GAL4/UAS experiments, animals were raised at 29 °C unless otherwise stated. Larvae hatching within a 2 hr window were transferred to cornmeal food (5.9% Glucose, 6.6% Cornmeal, 1.2% Baker's Yeast, 0.7% Agar in water) or NR medium (5% Sucrose, 1% Agar in PBS) and further synchronised by selecting L2 larvae morphologically from an L1/L2 moulting population. For EdU experiments, dissected CNSs were incubated for 1 hr in 10 μM EdU/PBS, fixed for 15 min in 4 % Formaldehyde/PBS and Alexa Fluor azide detected according to instructions (Click-iT EdU Imaging Kit, Invitrogen). CNS explants were cultured on 8μm pore-size inserts in Schneider's medium-10% fetal calf serum, 2mM L-glutamine (Gibco) and 1x Pen Strep (Gibco)- in 24-well Transwell plates (Costar) in a humidified chamber at 25 °C. For EdU quantifications, the "thoracic" region used corresponds to the ventral nerve cord from the level of the brain-lobes down to A1/A2 (Fig. 1a). $EdU^+$ voxels were quantified using Volocity (Improvision) from an average of 10 CNSs per experimental genotype, normalized to controls processed in parallel (siblings or half-siblings), using Leica SP5 scans (LAS AF software) with a 1.5 μm-step z-series. For larval mass measurements, triplicates of ~50 wandering L3 male larvae per genotype were transferred to pre-weighed microfuge tubes and wet weights determined using a Precisa XB 120A balance. For all histograms, error bars represent the s.e.m. and p values are from two-tailed Student *t*-tests with equal sample variance. Further details can be found in full Methods section.

## METHODS

### Rearing and staging of *Drosophila* larvae

To assist larval genotyping, lethal chromosomes were re-established over *Dfd-YFP* balancers. For EdU experiments, crosses were performed in cages with grape-juice plates (25% (v/v) grape-juice, 1.25% (w/v) sucrose, 2.5% (w/v) agar) supplemented with live yeast paste. For GAL4/UAS experiments, larvae hatched within a 2 hr time-window were transferred to our standard cornmeal food (5.9% w/v Glucose, 6.6% Cornmeal, 1.2% Baker's Yeast, 0.7% Agar in water) or to NR medium (5% Sucrose, 1% Agar in PBS). Animals were raised at 29 °C throughout, with the following exceptions due to lethality at high temperature: *tub-GAL80$^{ts}$,Repo>shi$^{DN}$* and *tub-GAL80$^{ts}$,Repo>Ilp2* animals were raised at 25 °C during embryogenesis and 29 °C during larval development, other *Ilp2*

overexpressions were performed at 25 °C throughout. At the time of dissection, development was further synchronised by selecting L2 animals morphologically from a mixed L1/L2 moulting population. *Df(3L)[Ilps2-3],Ilp5* and *Df(3L)[Ilps1-5]* animals develop considerably slower than controls, so EdU-incorporation experiments utilized morphological staging after the L1/L2 and L2/L3 moults. Co-expression of *Dcr-2* was used to enhance knockdown efficiency for the $Slif^{ANTI}$ antisense EP allele. As absolute numbers of reactivated neuroblasts can vary with small differences in temperature and humidity, parallel control experiments were carried out for each genetic background (using the siblings or half-siblings of experimental animals), rather than using a single control.

## *Drosophila* strains

Stocks used in this study were: $Tor^{2L19}$ (Ref. 31), $InR^{31}$ (Ref. 32), *Df(3L)[Ilps1-5]*, *Df(X)[Ilp6]* and *Df(X)[Ilp7]* (Ref. 33), $Ilp1^{1}$, $Ilp2^{1}$ $Ilp3^{1}$ $Ilp4^{1}$ $Ilp5^{1}$ $Df(X)Ilp6^{61}$, $Df(X)Ilp6^{68}$, $Ilp7^{1}$, *Df(3L)[Ilps2-3]*, *Df(3L)[Ilps2-3],Ilp5*$^{3}$, *Df(3L)[Ilps1-4],Ilp5*$^{3}$ (Ref. 34), $UAS\text{-}slif^{ANTI}$ (Ref. 35), *UAS-TSC1/2* (Ref. 36), *UAS-Rheb*, $UAS\text{-}InR^{DN} = UAS\text{-}InR^{K1409A}$, $UAS\text{-}InR^{ACT} = UAS\text{-}InR^{A1325D}$, FB driver = *Cg-GAL4* (Ref. 37), pan-glial driver = *Repo-GAL4* (Ref. 38), *OK107-GAL4* (Ref. 39), *eg-GAL4* (Ref. 40), *DopR-GAL4* (Ref. 41), *btl-GAL4* (Ref. 42), *UAS-CD8::GFP, FRT82B*, $tub\text{-}GAL80^{ts}$, *Sco/CyO,Dfd-YFP* and *Dr/TM6B,Sb,Dfd-YFP* (Bloomington *Drosophila* Stock Center), $UAS\text{-}Dp110^{DN} = UAS\text{-}Dp110^{A2860C}$ and $UAS\text{-}Dp110^{ACT} = UAS\ Dp110^{CAAX}$ (Ref. 43), *UAS-PTEN* (Ref. 44), *UAS-p60* (Ref. 45), $UAS\text{-}PDK^{ACT} = UAS\text{-}Pdk1^{A467V}$ (Ref. 46), *UAS-foxo.P* (Ref. 47), *UAS-Dcr2* (VDRC), *UAS-Ilp7* (Ref. 48), *UAS-Ilp1*, *UAS-Ilp2*, *UAS-Ilp3*, *UAS-Ilp4*, *UAS-Ilp5*, *UAS-Ilp6, Ilp3-nLacZ*$^{pXD311\text{-}1}$ and *Ilp3-nLacZ*$^{pXD311\text{-}11}$ (both recapitulate endogenous *Ilp3* expression in L3 mNSCs, Ref. 49), $UAS\text{-}shi^{DN}$ (Ref. 50), NB driver = $nab\text{-}GAL4^{NP4604}$ (Ref. 51), cortex glia driver = *NP577-GAL4* and ensheathing glia driver = *NP6520-GAL4* (Ref. 52), *Ilp6-GAL4 = NP1079-GAL4* (NIG stock centre), Subperineurial BBB glia driver = *Moody-GAL4* (Ref. 53), midline glia driver = *slit-GAL4* (Ref. 54), midline glia/neuronal driver = *sim-GAL4* (Ref. 55), mNSC driver = *Ilp2-GAL4* (Ref. 56), pan-neuronal driver = *n-syb-GAL4* (Ref. 57), *Ubx-GAL4* (Ref. 58), *wg-GAL4* (Ref. 59), *en-GAL4* was a gift from A. Brand via Jean-Paul Vincent, *Repo-FLP* (Ref. 60).

## EdU detection, immunostaining, *in situ* hybridization and imaging

L1 and L2 tissues were immobilised on poly-L-Lysine-coated slides for all stainings, except for CNS explants. For EdU experiments, dissected CNSs were incubated for 1 hr in 10 μM EdU/PBS, fixed for 15 min in 4 % Formaldehyde/PBS, followed by detection of Alexa Fluor azide according to the manufacturer's instructions (Click-iT EdU Imaging Kit, Invitrogen) and washing in 0.1% Triton/PBS. Antibody staining and *in situ* hybridisation were performed according to standard protocols. Primary antibodies used in this study were: rabbit anti-β-Galactosidase (Molecular Probes) 1/2000; rabbit anti-GFP (Invitrogen) 1/1000; mouse anti-Repo 1/20; mouse anti-Miranda 1/20 and rat anti-Elav 1/100 (Developmental Studies Hybridoma Bank); pre-adsorbed Alkaline Phosphatase-conjugated sheep anti-Digoxigenin 1/2000. Secondary antibodies used were: $F(ab')_2$ fragments conjugated to either Alexa-Fluor-488, Alexa-Fluor-633 (Molecular Probes) or Cy3 (Jackson), used at 1/250-1/2000. Live tissues were photographed in PBS. Fixed tissues labeled for fluorescence microscopy were mounted in Vectashield (Vector Laboratories) whereas those processed for *in situ* hybridisation were mounted in 80% Glycerol. Fluorescent images were acquired with a Leica SP5 confocal microscope (LAS AF software) and bright-field images were acquired with a Zeiss Axiophot2 microsope (AxioVision software). Images of the whole CNS are projections of a 1.5 μm-step z-series. Images of fat body and of high-magnification double-labels of parts of the CNS are single sections except for the right panel of Fig. 3e, which is a projection of 13 sections from a z-series.

### CNS Explant cultures

Explanted CNSs from larvae hatched within a 2hr window were cultured for 3-4 days on 8μm pore-size inserts in 10 μM EdU in Schneider's medium, 10% fetal calf serum, 2mM L-glutamine (Gibco) and 1x Pen Strep (Gibco), in 24-well Transwell plates (Costar) placed in a humidified chamber at 25 °C.

### Quantification of EdU incorporation

The “thoracic” region used for EdU quantifications corresponds to the ventral nerve cord from brain-lobe level down to A1/A2, distinguishable from more posterior neuromeres by a sharp transition in neuroblast density (Fig. 1a). The numbers of $EdU^+$ voxels per CNS were determined using Volocity (Improvision) from Leica SP5 confocal microscope scans (LAS AF software) using a 1.5 μm-step z-series. An average of 10 CNSs were quantified per experimental genotype and controls (siblings or half-siblings) were processed in parallel. Control and experimental values were normalized using the average number of control $EdU^+$ voxels. For all histograms, error bars represent standard error of the mean (s.e.m) of normalised values and asterisks indicate $p<0.05$ using two-tailed Student *t*-tests with equal sample variance.

### Larval mass measurements

Wet weights were determined for wandering L3 male larvae, sexed and genotyped in PBS, dabbed dry with tissue and transferred to pre-weighed microfuge tubes. For each data point, triplicate samples, each containing an average of 50 animals per genotype were weighed (Precisa XB 120A balance).

## METHODS REFERENCES


31. Oldham S, et al. Genetic and biochemical characterization of dTOR, the Drosophila homolog of the target of rapamycin. Genes Dev. 2000; 14(21):2689. [PubMed: 11069885]
32. Brogiolo W, et al. An evolutionarily conserved function of the Drosophila insulin receptor and insulin-like peptides in growth control. Curr Biol. 2001; 11(4):213. [PubMed: 11250149]
33. Zhang H, et al. Deletion of Drosophila insulin-like peptides causes growth defects and metabolic abnormalities. Proc Natl Acad Sci U S A. 2009; 106(46):19617. [PubMed: 19887630]
34. Gronke S, et al. Molecular evolution and functional characterization of Drosophila insulin-like peptides. PLoS Genet. 2010; 6(2):e1000857. [PubMed: 20195512]
35. Colombani J, et al. A nutrient sensor mechanism controls Drosophila growth. Cell. 2003; 114(6): 739. [PubMed: 14505573]
36. Tapon N, et al. The Drosophila tuberous sclerosis complex gene homologs restrict cell growth and cell proliferation. Cell. 2001; 105(3):345. [PubMed: 11348591]
37. Hennig KM, Colombani J, Neufeld TP. TOR coordinates bulk and targeted endocytosis in the Drosophila melanogaster fat body to regulate cell growth. J Cell Biol. 2006; 173(6):963. [PubMed: 16785324]
38. Xiong, et al. repo encodes a glial-specific homeo domain protein required in the Drosophila nervous system. Genes Dev. 1994; 8:981. [PubMed: 7926782]
39. Connolly, et al. Associative learning disrupted by impaired Gs signaling in Drosophila mushroom bodies. Science. 1996; 274(5295):2104. [PubMed: 8953046]
40. Ito K, Urban J, Technau GM. Distribution, classification, and development of Drosophila glial cells in the late embryonic and early larval ventral nerve cord. Rouxs Arch Dev Biol. 1995; 204(5):284.
41. Hacker U, et al. piggyBac-based insertional mutagenesis in the presence of stably integrated P elements in Drosophila. PNAS. 2003; 100(13):7720. [PubMed: 12802016]
42. Shiga Y, Tanaka-Matakatsu M, Hayashi S. A nuclear GFP/ beta-galactosidase fusion protein as a marker for morphogenesis in living Drosophila. Dev Growth Diff. 1996; 38(1):99.

43. Leevers SJ, et al. The Drosophila phosphoinositide 3-kinase Dp110 promotes cell growth. EMBO J. 1996; 15(23):6584. [PubMed: 8978685]
44. Huang H, et al. PTEN affects cell size, cell proliferation and apoptosis during Drosophila eye development. Development. 1999; 126(23):5365. [PubMed: 10556061]
45. Weinkove D, et al. Regulation of imaginal disc cell size, cell number and organ size by Drosophila class I(A) phosphoinositide 3-kinase and its adaptor. Curr Biol. 1999; 9(18):1019. [PubMed: 10508611]
46. Rintelen F, Stocker H, Thomas G, Hafen E. PDK1 regulates growth through Akt and S6K in Drosophila. Proc Natl Acad Sci U S A. 2001; 98(26):15020. [PubMed: 11752451]
47. Puig O, Marr MT, Ruhf ML, Tjian R. Control of cell number by Drosophila FOXO: downstream and feedback regulation of the insulin receptor pathway. Genes Dev. 2003; 17(16):2006. [PubMed: 12893776]
48. Miguel-Aliaga I, Thor S, Gould AP. Postmitotic specification of Drosophila insulinergic neurons from pioneer neurons. PLoS Biol. 2008; 6(3):e58. [PubMed: 18336071]
49. Ikeya T, et al. Nutrient-dependent expression of insulin-like peptides from neuroendocrine cells in the CNS contributes to growth regulation in Drosophila. Curr Biol. 2002; 12(15):1293. [PubMed: 12176357]
50. Moline MM, Southern C, Bejsovec A. Directionality of wingless protein transport influences epidermal patterning in the Drosophila embryo. Development. 1999; 126(19):4375. [PubMed: 10477304]
51. Maurange C, Cheng L, Gould AP. Temporal transcription factors and their targets schedule the end of neural proliferation in Drosophila. Cell. 2008; 133(5):891. [PubMed: 18510932]
52. Awasaki T, Lai S-L, Ito K, Lee T. Organization and Postembryonic Development of Glial Cells in the Adult Central Brain of Drosophila. J Neurosci. 2008; 28(51):13742. [PubMed: 19091965]
53. Schwabe T, et al. GPCR Signaling Is Required for Blood-Brain Barrier Formation in Drosophila. Cell. 1995; 123(1):133. [PubMed: 16213218]
54. Scholz H, Sadlowski E, Klaes A, Klambt C. Control of midline glia development in the embryonic *Drosophila* CNS. Mech Dev. 1997; 64:137. [PubMed: 9232604]
55. Kidd T, Bland KS, Goodman CS. Slit is the midline repellent for the robo receptor in Drosophila. Cell. 1999; 96:785. [PubMed: 10102267]
56. Rulifson EJ, Kim SK, Nusse R. Ablation of insulin-producing neurons in flies: growth and diabetic phenotypes. Science. 2002; 296(5570):1118. [PubMed: 12004130]
57. Pospisilik JA, et al. Drosophila genome-wide obesity screen reveals hedgehog as a determinant of brown versus white adipose cell fate. Cell. 2010; 140(1):148. [PubMed: 20074523]
58. de Navas LF, Garaulet DL, Sanchez-Herrero E. The ultrabithorax Hox gene of Drosophila controls haltere size by regulating the Dpp pathway. Development. 2006; 133(22):4495. [PubMed: 17050628]
59. Pfeiffer S, Alexandre C, Calleja M, Vincent JP. The progeny of wingless-expressing cells deliver the signal at a distance in Drosophila embryos. Curr Biol. 2000; 10(6):321. [PubMed: 10744976]
60. Silies M, Yuva Y, Engelen D, Aho A, Stork T, Klämbt C. Glial cell migration in the eye disc. J Neurosci. 2007; 27(48):13130. [PubMed: 18045907]


## Supplementary Material

Refer to Web version on PubMed Central for supplementary material.

## Acknowledgments

We are grateful to Andrea Brand, Steve Cohen, Bruce Edgar, Ulrike Gaul, Ernst Hafen, Christian Klambt, Tzumin Lee, Sally Leevers, Pierre Leopold, Fumio Matsuzaki, Irene Miguel-Aliaga, Tom Neufeld, Ruth Palmer, Linda Partridge, Leslie Pick, Ernesto Sanchez-Herrero, Hugo Stocker, Nic Tapon, Tian Xu, and also to the Bloomington stock centre and Kyoto National Institute of Genetics (NIG) for fly stocks, antibodies and plasmids. We also acknowledge Iris Salecker, Jean-Paul Vincent, Andrew Bailey, Einat Cinnamon, Louise Cheng, Rami Makki, Ander Matheu, Panayotis Pachnis, Patricia Serpente and Irina Stefana for providing advice, reagents and critical reading of the manuscript. Authors were supported by the Medical Research Council (U117584237).

## REFERENCES


1. Dhawan J, Rando TA. Stem cells in postnatal myogenesis: molecular mechanisms of satellite cell quiescence, activation and replenishment. Trends Cell Biol. 2005; 15:666–73. [PubMed: 16243526]
2. Coller HA. What's taking so long? S-phase entry from quiescence versus proliferation. Nat Rev Mol Cell Biol. 2007; 8:667–70. [PubMed: 17637736]
3. Yanagida M. Cellular quiescence: are controlling genes conserved? Trends Cell Biol. 2009; 19:705–715. [PubMed: 19833516]
4. Chen E, Finkel T. Preview. The Tortoise, the hare, and the FoxO. Cell Stem Cell. 2009; 5:451–2. [PubMed: 19896431]
5. Sanchez-Garcia I, Vicente-Duenas C, Cobaleda C. The theoretical basis of cancer-stem-cell-based therapeutics of cancer: can it be put into practice? Bioessays. 2007; 29:1269–80. [PubMed: 18022789]
6. Betschinger J, Knoblich JA. Dare to be different: asymmetric cell division in Drosophila, C. elegans and vertebrates. Curr Biol. 2004; 14:R674–85. [PubMed: 15324689]
7. Egger B, Chell JM, Brand AH. Insights into neural stem cell biology from flies. Philos Trans R Soc Lond B Biol Sci. 2008; 363:39–56. [PubMed: 17309865]
8. Doe CQ. Neural stem cells: balancing self-renewal with differentiation. Development. 2008; 135:1575–87. [PubMed: 18356248]
9. Sousa-Nunes R, Cheng LY, Gould AP. Regulating neural proliferation in the Drosophila CNS. Curr Opin Neurobiol. 2010; 20:50–7. [PubMed: 20079625]
10. Truman JW, Bate M. Spatial and temporal patterns of neurogenesis in the central nervous system of Drosophila melanogaster. Dev Biol. 1988; 125:145–57. [PubMed: 3119399]
11. Tsuji T, Hasegawa E, Isshiki T. Neuroblast entry into quiescence is regulated intrinsically by the combined action of spatial Hox proteins and temporal identity factors. Development. 2008; 135:3859–69. [PubMed: 18948419]
12. Kambadur R, et al. Regulation of POU genes by castor and hunchback establishes layered compartments in the Drosophila CNS. Genes Dev. 1998; 12:246–60. [PubMed: 9436984]
13. Isshiki T, Pearson B, Holbrook S, Doe CQ. Drosophila neuroblasts sequentially express transcription factors which specify the temporal identity of their neuronal progeny. Cell. 2001; 106:511–21. [PubMed: 11525736]
14. Britton JS, Edgar BA. Environmental control of the cell cycle in Drosophila: nutrition activates mitotic and endoreplicative cells by distinct mechanisms. Development. 1998; 125:2149–58. [PubMed: 9570778]
15. Colombani J, et al. A nutrient sensor mechanism controls Drosophila growth. Cell. 2003; 114:739–49. [PubMed: 14505573]
16. Brogiolo W, et al. An evolutionarily conserved function of the Drosophila insulin receptor and insulin-like peptides in growth control. Curr Biol. 2001; 11:213–21. [PubMed: 11250149]
17. Ikeya T, Galic M, Belawat P, Nairz K, Hafen E. Nutrient-dependent expression of insulin-like peptides from neuroendocrine cells in the CNS contributes to growth regulation in Drosophila. Curr Biol. 2002; 12:1293–300. [PubMed: 12176357]
18. Rulifson EJ, Kim SK, Nusse R. Ablation of insulin-producing neurons in flies: growth and diabetic phenotypes. Science. 2002; 296:1118–20. [PubMed: 12004130]
19. Slaidina M, Delanoue R, Gronke S, Partridge L, Leopold P. A Drosophila insulin-like peptide promotes growth during nonfeeding states. Dev Cell. 2009; 17:874–84. [PubMed: 20059956]
20. Okamoto N, et al. A fat body-derived IGF-like peptide regulates postfeeding growth in Drosophila. Dev Cell. 2009; 17:885–91. [PubMed: 20059957]
21. Geminard C, Rulifson EJ, Leopold P. Remote control of insulin secretion by fat cells in Drosophila. Cell Metab. 2009; 10:199–207. [PubMed: 19723496]
22. Polak P, Hall MN. mTOR and the control of whole body metabolism. Curr Opin Cell Biol. 2009; 21:209–18. [PubMed: 19261457]
23. Neufeld TP. Body building: regulation of shape and size by PI3K/TOR signaling during development. Mech Dev. 2003; 120:1283–96. [PubMed: 14623438]

24. Teleman AA. Molecular mechanisms of metabolic regulation by insulin in Drosophila. Biochem J. 2010; 425:13–26. [PubMed: 20001959]

25. Gronke S, Clarke DF, Broughton S, Andrews TD, Partridge L. Molecular evolution and functional characterization of Drosophila insulin-like peptides. PLoS Genet. 2010; 6:e1000857. [PubMed: 20195512]

26. Zhang H, et al. Deletion of Drosophila insulin-like peptides causes growth defects and metabolic abnormalities. Proc Natl Acad Sci U S A. 2009; 106:19617–22. [PubMed: 19887630]

27. Chell JM, Brand AH. Nutrition-responsive glia control exit of neural stem cells from quiescence. Cell. 2010; 143:1161–73. [PubMed: 21183078]

28. Mangan S, Alon U. Structure and function of the feed-forward loop network motif. Proc Natl Acad Sci U S A. 2003; 100:11980–5. [PubMed: 14530388]

29. Fernandez-Almonacid R, Rosen OM. Structure and ligand specificity of the Drosophila melanogaster insulin receptor. Mol Cell Biol. 1987; 7:2718–27. [PubMed: 3118188]

30. Hodge RD, D'Ercole AJ, O'Kusky JR. Insulin-like growth factor-I accelerates the cell cycle by decreasing G1 phase length and increases cell cycle reentry in the embryonic cerebral cortex. J Neurosci. 2004; 24:10201–10. [PubMed: 15537892]

Europe PMC Funders Author Manuscripts

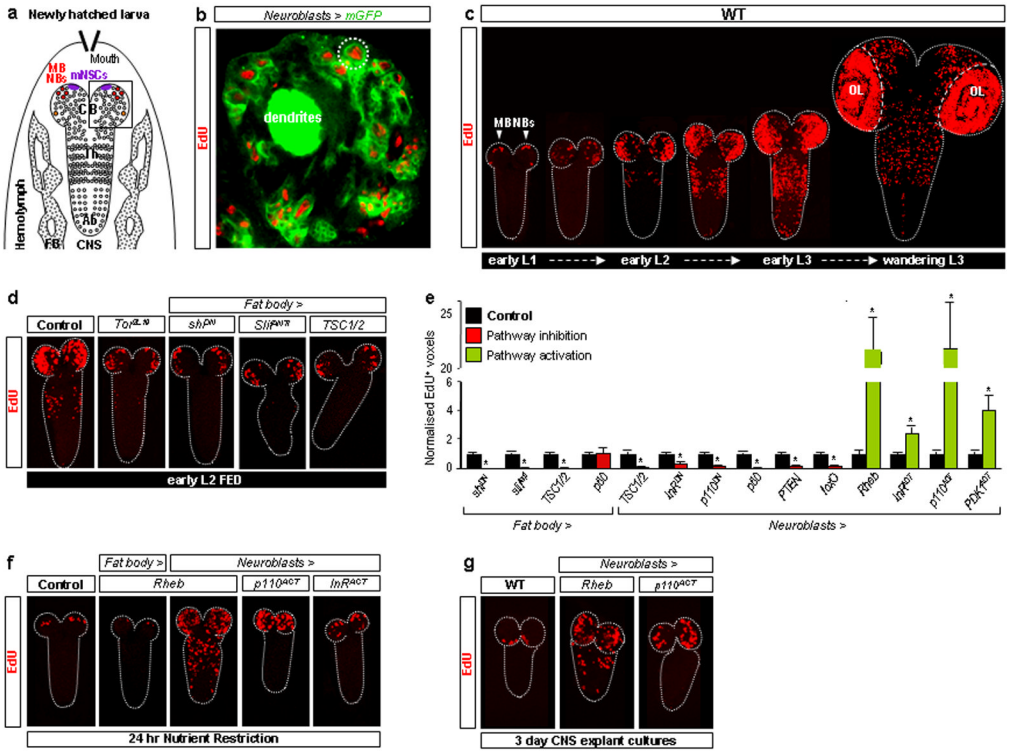


**Fig. 1. TOR/PI3K signalling in fat body and neuroblasts regulates reactivation**

**a**, Diagram depicting larval fat body (FB) and CNS with central brain (CB), thoracic (Th) and abdominal (Ab) neuromeres, mNSCs, mushroom body (MB NBs) and other neuroblasts (circles) indicated. **b**, Brain lobe (inset in Fig.1a), showing EdU incorporation in postembryonic neuroblasts (large cells; e.g dotted circle) and their progeny (smaller cells), labelled with *nab-GAL4* driving membrane GFP (*Neuroblasts>mGFP*). **c**, EdU incorporation timecourse from first-instar (L1) to third-instar (L3) larval stages in the wild-type (WT) CNS (OL, optic lobes). **d,f,g**, EdU-labelled CNSs from larvae expressing TOR/PI3K components driven by *Cg-GAL4* (*Fat body>*) or *nab-GAL4* (*Neuroblasts>*). **e**, Histograms of $EdU^+$ voxels from thoracic CNSs of fed larvae, normalized to controls. In this and all subsequent figures, error bars are s.e.m.; * $p<0.05$. See text, Methods and Supplementary Fig. 2 for details of molecules expressed.




Europe PMC Funders Author Manuscripts

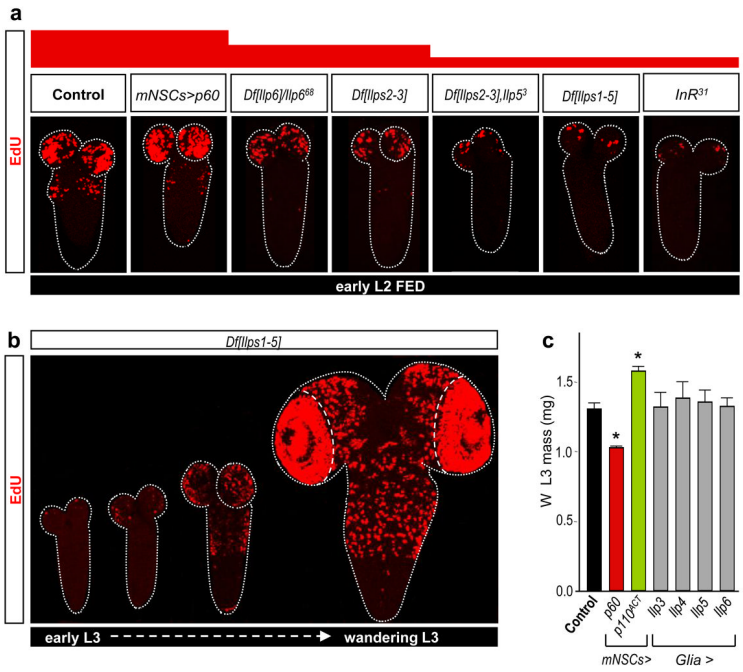


**Fig. 2. Insulin-like peptides but not mNSCs control neuroblast reactivation**

**a**, EdU-labelled CNSs from various *Ilp* or *InR* mutants show decreased reactivation whereas larvae with *Ilp2-GAL4* driving *UAS-p60* (*mNSC>p60*) do not. **b**, EdU incorporation timecourse in the CNS of *Df[Ilps1-5]* larvae. **c**, The mass of fed L3 larvae at the wandering (W) stage is significantly altered by *Ilp2-GAL4* (*mNSC>*) driving PI3K signalling components but not by *repo-GAL4* (*Glia>*) driving Ilps.




Europe PMC Funders Author Manuscripts

Europe PMC Funders Author Manuscripts

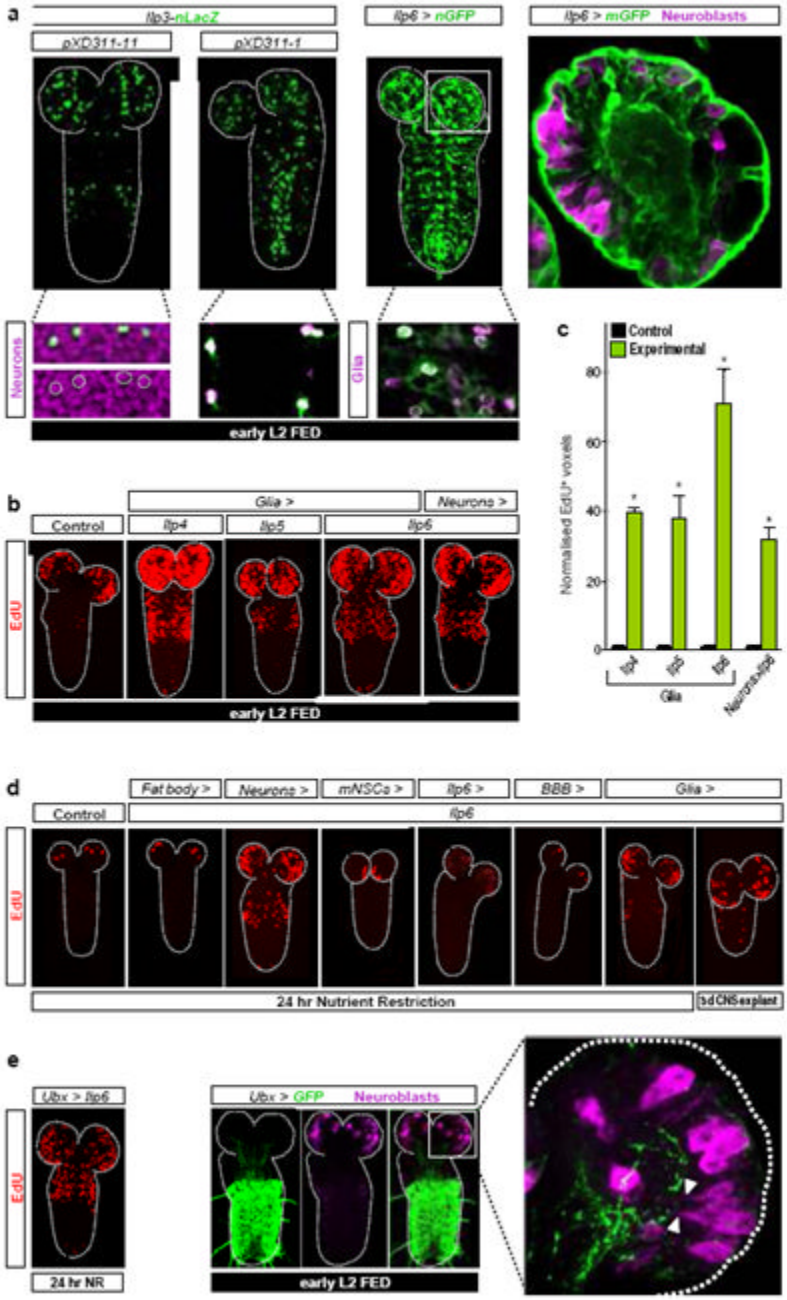


**Fig. 3. CNS-specific Ilps are sufficient for neuroblast reactivation**

**a**, Panels show expression of *Ilp3-nLacZ* in subsets of neurons (*XD311-11*) and glia (*XD311-1*) and *Ilp6-GAL4* (*Ilp6>nGFP* and *Ilp6>mGFP*) in glia, including BBB surface and cortex glia. **b**,**d** EdU-labelled CNSs from larvae overexpressing *Ilps* in various cell types (see Methods for GAL4 drivers used). **c**, Histograms of normalized $EdU^+$ voxels in the thoracic CNS for the genotypes in b. **e**, *Ilp6* overexpression in the *Ultrabithorax* domain (*Ubx>Ilp6*) reactivates neuroblasts in the normal spatial pattern during NR (left panel). Quiescent/enlarging neuroblasts in the central brain, far from the posterior *Ubx* domain (middle panels), extend cytoplasmic processes (arrowheads) towards the neuropil, close to long $Ubx^+$ cell processes (right panel). The range of Ilp6 activity is difficult to determine

from this experiment. Neurons, glia and neuroblasts are marked by Elav, Repo and Miranda respectively.



Europe PMC Funders Author Manuscripts

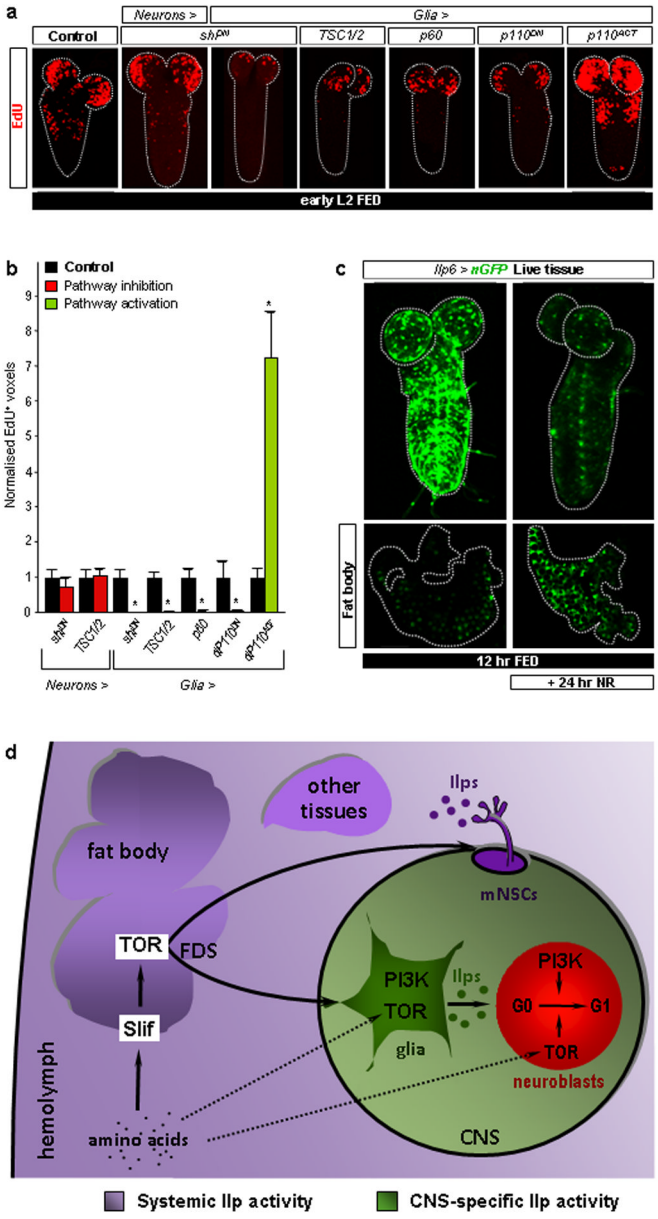


**Fig. 4. Ilp6-expressing glia are nutritionally regulated**

**a**, EdU-labelled CNSs from larvae expressing the components indicated. **b**, Histograms of normalized EdU$^{+}$ voxels in the thoracic CNS for genotypes in a. **c**, *Ilp6*>nGFP expression in the CNS and fat body of fed versus NR larvae. **d**, Relay model for amino-acid dependent fat body regulation of CNS and body growth. CNS-restricted (green) and systemic (purple) pools of Insulin-like peptides (Ilps) are functionally segregated. Direct amino-acid sensing by glia and neuroblasts may contribute to neuroblast reactivation (dashed arrows). See text for details.




Europe PMC Funders Author Manuscripts